Dalton Transactions

ROYAL SOCIETY OF CHEMISTRY

PAPER

View Article Online
View Journal | View Issue

Cite this: *Dalton Trans.*, 2024, **53**, 14226

pK_{aH} values and θ_H angles of phosphanes to predict their electronic and steric parameters†

Marta-Lisette Pikma, Sofja Tshepelevitsh, Sigrid Selberg, Ivari Kaljurand, Ivo Leito and Agnes Kütt *

Received 15th May 2024,
Accepted 5th August 2024

DOI: 10.1039/d4dt01430h

rsc.li/dalton

Phosphanes play an important role in various applications, serving as a class of organic bases with basicities spanning more than 30 orders of magnitude. Accessing comprehensive basicity data for phosphanes has been challenging due to scattered information across multiple sources and notable gaps in the existing data. In this report, we present basicities (pK_{aH} values) of a diverse set of phosphanes, both newly measured or calculated and collected from the literature. We demonstrate that pK_{aH} values can serve as an alternative to Tolman electronic parameters (TEP values) in evaluating the electronic properties of phosphanes. Additionally, we suggest parameters for assessing the steric properties of phosphanes without the need for preparation or calculation of metal-ligand complexes.

Introduction

The adaptable reactivity of phosphanes makes them indispensable across various chemistry disciplines, spanning organic synthesis, materials science, pharmaceuticals, and beyond. Phosphanes are widespread ligands in homogeneous transition metal catalysis, facilitating a wide range of organic transformations such as hydrogenation, cross-coupling reactions (*e.g.*, Heck reaction, Buchwald-Hartwig amination, Suzuki-Miyaura coupling, *etc.*), olefin metathesis, three-component coupling reactions, polymerization, asymmetric synthesis, Michael addition, Wittig reactions, *etc.*[1–9] Bulky phosphanes are also commonly employed in frustrated Lewis pair (FLP) systems as Lewis bases for activating small molecules and non-transition metal catalysis.[10]

Phosphanes offer several advantages over possible alternative reagents (*e.g.*, N-heterocyclic carbenes,[11] nitrogen-containing ligands,[12] *etc.*): they are straightforward to synthesize, many are stable under ordinary environmental conditions, and are often commercially available. Furthermore, their properties can be adjusted to suit the requirements of a particular catalytic transformation, rendering them a favored option for ligands. To facilitate extensive ligand screening for catalytic transformations, several databases have been developed, such as the Ligand Knowledge Base (LKB), which comprises computed properties for a wide range of phosphanes, as well as the Kraken discovery platform, among others.[13,14]

Although phosphanes are primarily used in metal complexes, some of them, particularly those substituted with aromatic rings carrying *para*/*ortho* MeO groups, have found independent applications as catalysts as well, owing to their basic characteristics.[15,16] Given the widespread application of phosphanes as nucleophiles and the possibility to predict their related properties based on their basicity,[17] phosphanes as bases have been well studied, resulting in the availability of numerous reported pK_{aH} values.[18–20] However, despite these advancements, there are still notable gaps in this field, emphasizing the need for further investigations.

In the current work, we present self-consistent experimental pK_{aH} values of 25 phosphanes, measured using relative UV-Vis and NMR methods. Some of the phosphanes are known to have high basicity but their exact pK_{aH} values are presented for the first time. COSMO-RS method was used to predict pK_{aH} values for the 21 phosphanes that were not studied experimentally.

The basicity of a base B in a solvent is defined by equilibrium (1); the pK_{aH} value of a base B is equivalent to the pK_a of its conjugate acid BH^+ and is the negative logarithm of the conjugated acid's dissociation constant K_a (eqn (2)).

$$BH^+ + S \overset{K_a}{\rightleftarrows} B + HS^+ \quad (1)$$

$$K_a = \frac{a(HS^+)a(B)}{a(BH^+)} \quad (2)$$

The gas-phase basicity (GB) of a neutral base B refers to the following equilibrium:

$$B + H^+ \overset{GB}{\rightleftarrows} BH^+ \quad (3)$$

Institute of Chemistry, University of Tartu, Ravila 14a, Tartu 50411, Estonia. E-mail: agnes.kutt@ut.ee

†Electronic supplementary information (ESI) available. See DOI: https://doi.org/10.1039/d4dt01430h

GB of a base is the negative of Gibbs free energy change ($-\Delta G_b$) on protonation of the base according to equilibrium (3). Differently from proton affinity (PA), GB values include the entropy factor.

Electronic and steric parameters of ligands, a concept first introduced by C.A. Tolman in the 1970s, have been used to describe phosphanes.[21,22] The Tolman electronic parameter (TEP) and Tolman cone angle are still the most commonly used characteristics in ligand chemistry.

TEP values of phosphanes as ligands are often determined by the infrared vibration of the CO group in ligand-Ni(CO)$_3$ complexes (ν(CO)). While widely accepted and frequently applied to characterize new types of phosphanes due to their effectiveness in delineating electron-donating and accepting attributes of ligands, reliance on Ni(CO)$_4$ as a required starting compound poses challenges, as it is a toxic gas not readily available in most research laboratories. Additionally, computational determination of ν(CO) values for solvent-phase metal–ligand complexes can be resource-intensive and highly influenced by the solvent, rendering computational gas-phase values less reliable without a suitable reference system. Several alternatives exist for assessing ligands' electron-donating and -accepting properties in metal complexes. These alternatives include, *e.g.*, NBO analysis,[23] Hard-Soft Acid-Base (HSAB) Theory,[24] Local Vibrational Mode,[25] X-ray Crystallography,[26] *etc.*

Tolman cone angles were originally measured from metal-ligand complexes relatively robustly, using space-filling models and a specialized ruler; the distance from phosphorus to the metal was fixed to a length in the model equal to 2.28 Å on the molecular level.[22,27] This method undoubtedly involved generalizations concerning both the ligand conformation and the metal position. Tolman initially utilized the tightest conformer, a choice later contested by others as potentially inaccurate.[28,29] Hence, criticism has been directed towards the Tolman cone angle, and other approaches have been proposed.[30] For example, these include exact cone angles,[30] solid angles,[31] percent buried volumes (%V_{Bur}),[32,33] the He$_8$ steric descriptor in Ligand Knowledge Base (LKB),[13,34] angular symmetric deformation coordinate (S4′),[35,36] *etc.* Tolman cone angles have been recomputed for various phosphane ligands, which were obtained from three different transition metal coordination environments using the lowest-energy conformer geometry with MM/DFT methodology.[37] Steric parameters have been also derived not directly from the metal-ligand complex but from implied methods, *e.g.* by NMR spectroscopy,[38] organic reactivity,[39,40] *etc.*[41]

While modern parameters may offer greater precision in absolute values, they often prove inconvenient to obtain when only a rapid comparison of ligands is required. Therefore, employing a steric measure derived from a free ligand for preliminary screening holds promise for substantial resource savings.

While a number of parameters have been proposed to assess the electronic and steric properties of phosphanes, they are all derived from metal-ligand complexes, which is why the present study intended to investigate the feasibility of substituting these with alternative, more readily computed parameters for simple phosphanes as free ligands.

Results and discussion

In this work, experimental pK_{aH} values in acetonitrile were obtained for 12 phosphanes. Each compound was measured against at least 3 reference bases using a relative measurement method based on the UV-Vis or NMR spectra (see below).[42,43] In addition, pK_{aH}(MeCN) and GB values were calculated for a diverse set of phosphanes (see below and ESI†). The results from this work, in addition to values from the literature, are presented in Table 1. The structures of selected substituents are shown in Fig. 1.

As is seen from Table 1, electron-donating groups increase the basicity of phosphanes, whereas electron-accepting groups lower it. The elevation of basicity induced by the former arises from the stabilization of the protonated form, rendering the phosphane more inclined to accept a proton. In addition, despite the limited conjugation between the lone pair of phosphorus and the aromatic ring due to orbital positioning, a slight resonance effect remains, and electron-donating groups increase the accessibility of the lone pair on phosphorus in aromatic phosphanes.

Methoxy substituents in *ortho* and *para* positions increase the basicity of aryl-substituted phosphanes and lower it when in the *meta* position compared to PPh$_3$ (pK_{aH} value of PPh$_3$ is 7.62).[18,44] This is expected as the methoxy group is a resonance-donating group, and it increases the electron density in *para* and *ortho* positions (*i.e.*, increasing the electron density on the phosphorus, making the electron pair more available and also stabilizing the protonated phosphane). At the same time, the methoxy group is also an induction-acceptor group, thereby lowering the basicity when in the *meta* position.

Replacing unsubstituted phenyl rings with 2,4,6-methoxy substituted rings increases the basicity considerably. The basicity increase upon trimethoxy-substitution of one phenyl ring (PPh$_3$ (**35**) *vs.* P[2,4,6-(MeO)$_3$-C$_6$H$_2$]Ph$_2$ (**25**)) is 4.14 pK_{aH} units; substituting the second phenyl (**25** *vs.* P[2,4,6-(MeO)$_3$-C$_6$H$_2$]$_2$Ph (**8**)) causes about the same basicity increase (4.11 pK_{aH} units) and substituting the third phenyl (**8** *vs.* P[2,4,6-(MeO)$_3$-C$_6$H$_2$]$_3$ (**2**)) increases the pK_{aH} by another 3.79 units (Scheme 1). The minor reduction in the basicity increase for the latter is attributable to a saturation effect. Both P[2,4,6-(MeO)$_3$-C$_6$H$_2$]$_2$Ph (**8**) and P[2,6-(MeO)$_2$-C$_6$H$_3$]$_3$ (**6**) feature six methoxy groups; however, the latter exhibits a higher pK_{aH} value by approximately 1.5 units. This discrepancy suggests that the extra *ortho*-methoxy groups have an advantage over extra *para*-methoxy groups, as the former exert a more significant influence on basicity owing to their proximity to the protonation center in addition to the stabilization of the protonated form caused by the spatial proximity of the oxygen atoms to the proton.

Table 1 pK_{aH}(MeCN) values (computational, if not indicated otherwise) and GB values of phosphanes **1–56**. Tolman electronic parameters (TEP),[22] CPC angles (θ_{CPC}), exact cone angles for protonated phosphanes (θ_H) and average angles for Pd complexes with phosphane ligands (θ_{Pd}),[30] and Tolman cone angles (θ_{Tolman})[22] of phosphanes

No	Compound	pK_{aH}(MeCN) experimental	pK_{aH}(MeCN) computational	GB [kcal mol^{-1}]	TEP	θ_{CPC} [°]	θ_H [°]	θ_{Tolman} [°]	θ_{Pd} [°][i]
1	P(pyrr)$_3$	20.35[a]	19.5	241.8		111.7[f]	218		
2	P[2,4,6-(MeO)$_3$-C$_6$H$_2$]$_3$	19.66[b]	21.4	261.5		114.8	275		
3	P(dma)$_3$	18.9[a]	17.1	234.5	2061.9	111.6[f]	223	157	
4	PAd$_3$		18.5	246.2		115.0	244		
5	P(*t*-Bu)$_3$		17.3	238.1	2056.1	114.8	244	182	187.6
6	P[2,6-(MeO)$_2$-C$_6$H$_3$]$_3$	17.23[b]	18.2	254.2		114.8	273		
7	PCy$_3$	16.70[a]	16.6	240.3	2056.4	112.7	229	170	
8	P[2,4,6-(MeO)$_3$-C$_6$H$_2$]$_2$Ph	15.87[b]	16.5	252.6		114.0	252		
9	P(*i*-Pr)$_3$		15.7	233.1	2059.2	112.6	227	160	173.1
10	PMe$_2$Et		15.6	223.5		111.2	187	123	133.0
11	PMe$_3$	15.48[d]	15.6	221.4	2064.1	111.0	163	118	120.4
12	P(*i*-Pr)$_2$Me		15.3	228.6		111.9	219	146	160.1
13	PMeEt$_2$		15.1	225.4		111.4	187	127	141.4
14	P(*n*-Pr)$_3$		15.0	229.5		111.6	215	132	
15	PEt$_3$		14.8	226.8	2061.7	111.5	212	132	152.4
16	P(*n*-Bu)$_3$		14.7	230.0	2060.3	111.5	213	132	152.8
17	P(*t*-Bu)$_2$Ph		14.7	236.1		114.3	243	170	186.7
18	P(*i*-Bu)$_3$		13.8	229.7		110.9	250	143	213.8
19	PCy$_2$Ph		13.1	235.1		112.4	225	159	
20	PMes$_3$	12.87[b]	13.0	239.5		115.9	302	212	
21	PNp$_3$		12.8	231.3		110.0	284	180	
22	PEt$_2$Ph		12.7	228.2	2063.7	111.7	218	136	163.0
23	P(*n*-Bu)$_2$Ph		12.6	231.8		111.7	219	136	153.1
24	PMe$_2$Ph	12.64[d]	12.2	224.4	2065.3	111.2	198	122	148.5
25	P[2,4,6-(MeO)$_3$-C$_6$H$_2$]Ph$_2$	11.76[b]	11.5	241.5		113.2	237		
26	P(*t*-Bu)Ph$_2$		11.4	232.6		113.6	241	157	
27	PCyPh$_2$	10.23[b]	10.0	231.3		112.4	232	152	
28	PEtPh$_2$		10.1	227.3	2066.7	111.8	224	140	159.6
29	P(4-MeO-C$_6$H$_4$)$_3$	10.06[d]	10.5	239.5	2066.1	111.9	216	145	170.9
30	PMePh$_2$	9.97[e]	9.5	226.5	2067.0	111.4	202	136	151.4
31	P(2-MeO-C$_6$H$_4$)$_3$		9.8	241.4	2058.3	110.7	248		
32	PBn$_3$		9.3	229.1	2066.2	112.0	250	165	
33	P(4-Me-C$_6$H$_4$)$_3$		8.7	234.8	2066.7	111.7	216	145	170.7
34	P(2-Me-C$_6$H$_4$)$_3$		7.8	230.7	2066.6	111.7	277	194	191.9
35	PPh$_3$	7.62[d]	7.1	228.6	2068.9	111.6	218	145	170.0
36	P(1-Napht)Ph$_2$	7.29[b]	7.0	230.0		111.6	229		
37	P(3-MeO-C$_6$H$_4$)$_3$	7.25[b]	7.7	234.6		111.5	229		
38	P[3,5-(MeO)$_2$-C$_6$H$_3$]$_3$	7.19[b]	7.7	237.9		111.5	233		
39	P(4-F-C$_6$H$_4$)$_3$		6.7	224.0	2071.3	111.6	216	145	170.8
40	P(1-Napht)$_3$	6.55[e]	6.3	232.3		111.6	247		
41	P(2-F-C$_6$H$_4$)Ph$_2$	6.11[c]	5.9	227.5		111.3	222		
42	P(2,6-F$_2$-C$_6$H$_3$)Ph$_2$	5.17[c]	5.5	226.3		112.3	224		
43	P(4-Cl-C$_6$H$_4$)$_3$		4.9	223.3	2072.8	111.4	215	145	170.2
44	PPh$_2$H		4.7	216.7	2073.3	110.8[g]	187	128	146.3
45	P(2-F-C$_6$H$_4$)$_2$Ph	4.56[c]	4.5	225.3		111.1	227		
46	P(2-F-C$_6$H$_4$)$_3$	3.01[c]	3.0	224.1		110.7	231		
47	P(C$_6$F$_5$)Ph$_2$	2.54[c]	2.7	219.9	2074.8	112.2	225		
48	P(2,6-F$_2$-C$_6$H$_3$)$_2$Ph	2.50[c]	2.5	224.9		112.7	235		
49	P(2,6-Cl$_2$-C$_6$H$_3$)$_3$	1.70[c]	1.7	225.5		115.4	277		
50	P(2,6-F$_2$-C$_6$H$_3$)$_3$		0.5	222.0		113.5	255		
51	P[CH$_2$CH(CF$_3$)$_2$]$_3$		0.0	201.9		109.0	256		
52	PPh$_2$Cl		−0.2	212.5	2080.7	111.0[h]	202	138	156.3
53	P(C$_6$F$_5$)$_2$Ph		−2.0	211.1		112.3	234		
54	P[3,5-(CF$_3$)$_2$-C$_6$H$_3$]$_3$		−2.2	200.5		111.4	221		
55	P(CH$_2$CF$_3$)$_3$		−3.3	194.6		111.1	228		
56	P(C$_6$F$_5$)$_3$		−7.0	201.8	2090.9	113.0	253	184	

[a] Experimental value from this work (NMR). [b] Experimental value from this work (UV-Vis). [c] Experimental value from ref. 17. [d] Experimental value from ref. 18. [e] Experimental value from ref. 41. [f] NPN angles. [g] Including CPH angles. [h] Including CPCl angles. [i] In the case the angles for two conformers are available, the average angle is presented.

For the predicted pK_{aH}(MeCN) values presented in Table 1, the theoretical pK_{aH} values were initially computed with the COSMO-RS method[45,46] and then subsequently corrected using available experimental data pertaining to other phosphanes (calculation method described below). Different versions of COSMO-RS parameterizations may rely on distinct

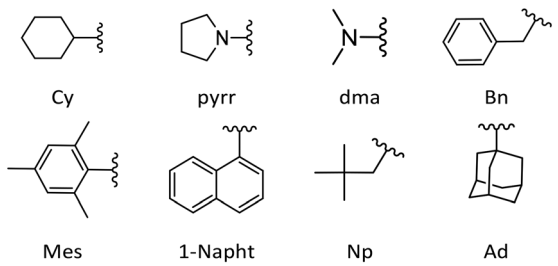

Fig. 1 Structures of some of the substituents of phosphanes in this work. Cy (cyclohexyl), pyrr (pyrrolidino), dma (dimethylamino), Bn (benzyl), Mes (mesityl), 1-Napht (1-naphthyl), Np (neopentyl), and Ad (adamantyl).

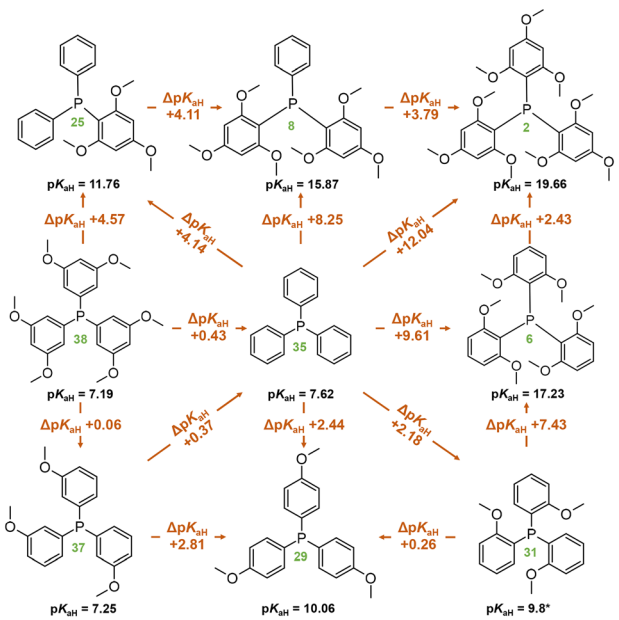

Scheme 1 Comparison of compounds with methoxyphenyl groups in terms of pK_{aH}(MeCN) values. Compound numbers, according to Table 1, are marked in green below the corresponding structures. *Predicted pK_{aH}(MeCN) value.

datasets, and while newer iterations generally demonstrate overall enhancement, their performance across predicted properties and compound classes can vary. Hence, it is beneficial to assess different parameterizations for a particular task. It was observed that the quality of the correlation between the calculated pK_{aH}(Calc.) (output of COSMOtherm software without additional corrections) and the experimental pK_{aH}(Exp.) depended markedly upon the COSMO-RS parameterization employed at a given level (TZVPD_FINE). Unexpectedly, more recent parameterizations yielded inferior results, both in terms of absolute values and the quality of correlation with the experiment. To discern the optimal parameterization, pK_{aH}(Calc.) values were computed with 8 parameterizations (Table 2).

The parameterization BP_TZVPD_FINE_C30_1701 from 2017 demonstrated the best correlation with experimental values and was consequently employed for the determination of predicted pK_{aH} values in this study. Nevertheless, in instances where the objective is the direct utilization of calculated values, the 2015 parameterization proves more advantageous, given its ability to yield a reduced root mean square deviation (Table 2). The correlation between calculated (pK_{aH}(Calc.)) and experimental (pK_{aH}(Exp.)) pK_{aH} values using BP_TZVPD_FINE_C30_1701 parameterization is depicted in Fig. 2. The correlation coefficient is reasonably high, and the slope of the correlation is statistically indistinguishable from 1. To obtain the predicted pK_{aH} values from computational pK_{aH} values for phosphanes, the following equation is used:

$$\begin{aligned} &\mathrm{p}K_{aH}(\mathrm{Exp.}) = 0.97(0.02)\cdot \mathrm{p}K_{aH}(\mathrm{Calc.}) + 1.1(0.3) \\ &n = 25; R^2 = 0.987;\ S = 0.673 \end{aligned} \quad (4)$$

It was also examined whether employing all conformers for pK_{aH} calculations yields significantly different results compared to using only the most stable conformer (denoted as c0). The average difference between these two is 0.08 units, and the largest deviating point (**34**) differs by around one pK_{aH} unit in absolute values. The correlation in Fig. 2 remains practically the same when using only the c0 conformer (Fig. 3). Considering the overall standard deviation of the correlation eqn (4), the predicted pK_{aH} values are not derived with substantially higher precision when using all conformers compared to using only the most stable one. Thus, in the case of predicting pK_{aH} values of phosphanes in MeCN, conformer searches at a lower level of theory and complete geometry calculation (geometry optimization at BP-TZVP level, frequency

Table 2 pK_{aH}(Calc.) *vs.* pK_{aH}(Exp.) correlation parameters for different parameterizations (n = 25; the solvent is MeCN, release year in parentheses)

Parameterization	Slope	R^2	S	RMSD
BP_TZVPD_FINE_23 (2023)	1.32 (0.07)	0.941	1.43	3.82
BP_TZVPD_FINE_20 (2020)	1.27 (0.06)	0.943	1.40	3.68
BP_TZVPD_FINE_18 (2018)	1.34 (0.06)	0.956	1.24	4.06
BP_TZVPD_FINE_C30_1701 (2017)	0.97 (0.02)	0.987	0.67	1.05
BP_TZVPD_FINE_ C30_1601 (2016)	1.00 (0.03)	0.980	0.84	0.84
BP_TZVPD_FINE_ C30_1501 (2015)	1.00 (0.03)	0.979	0.86	0.83
BP_TZVPD_FINE_ C30_1401 (2014)	1.02 (0.04)	0.969	1.03	1.10
BP_TZVPD_FINE_HB2012_C30_1201 (2012)	1.04 (0.04)	0.964	1.12	1.30

The standard deviation for slope is in brackets. S – standard error for the correlation; RMSD – root mean square deviation between pK_{aH}(Calc.) and pK_{aH}(Exp.).

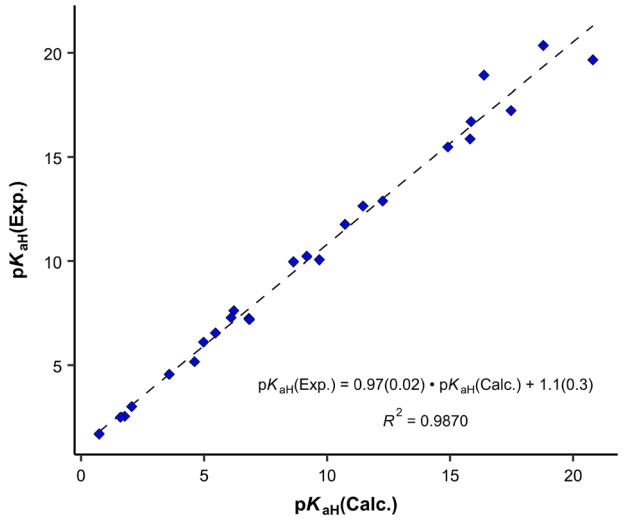

Fig. 2 Correlation between calculated and experimental pK_{aH}(MeCN) values.

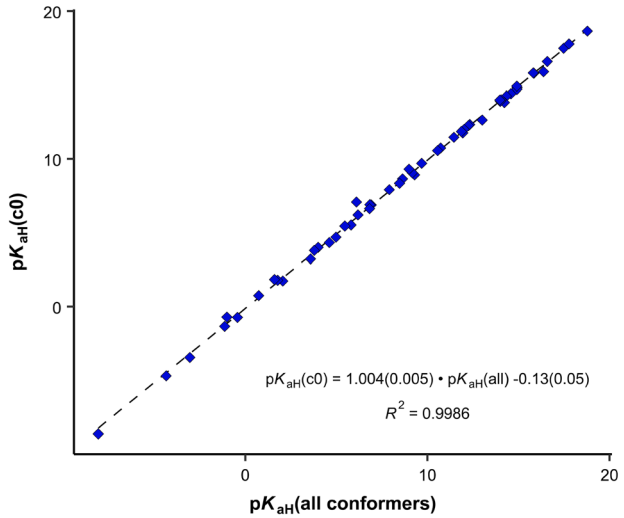

Fig. 3 Correlation between calculated pK_{aH} values using only the most stable conformer (c0) and all conformers.

calculation, and single-point calculation at BP-TZVPD level) only for the most stable structures (neutral and cation) can be considered to be sufficient.

The pK_{aH} value, a measure of the acidity of a hydrogen atom in a molecule, primarily reflects the electronic factors influencing the acidity/basicity center and is less affected by steric hindrance caused by more distant substituents. However, with substituents close to the protonation site, steric effects can sometimes significantly impact the stability of the protonated form and the accessibility of the hydrogen atom. For instance, in aromatic phosphanes, *ortho*-substitutions might engage in intramolecular hydrogen bonding with the proton, thereby significantly affecting the pK_{aH} value. Even in the absence of a hydrogen bond, *ortho*-substituents may offer additional stabilization of the protonated form. In the calculated structure of protonated P[2,6-(MeO)$_2$-C$_6$H$_3$]$_3$ (**6**), the distance between the proton and the oxygens in MeO groups is smaller (~2.45 Å) than the sum of their van der Waals radii (2.6 Å), suggesting the presence of some stabilizing effect, *e.g.*, electrostatic stabilization. However, this cannot be called a true intramolecular hydrogen bond as the H–O distance is too large and the P–H–O angle is very narrow (around 91°). Consequently, while pK_{aH} values offer insights into the electronic properties of compounds, they may not fully encompass the steric and structural factors.

Previously, the basicities of phosphanes and other ligands have already been utilized to predict electronic parameters and have been correlated with TEP values.[47,48] However, the dataset used was considerably limited in size. Given the ample availability of pK_{aH} values in our work, we can assess how effectively they mirror the donor and acceptor properties similar to TEP values (Fig. 4), eliminating the necessity to calculate or synthesize the actual metal-ligand complex. The correlation between pK_{aH}(MeCN) values and available TEP values (excluding three outliers, see below) is expressed by the following equation:

$$\begin{aligned} &\mathrm{TEP} = -1.34(0.05)\cdot \mathrm{p}K_{aH} + 2080(1) \\ &n = 20;\ R^2 = 0.977;\ S = 1.29 \end{aligned} \quad (5)$$

From the data available, three points stand out according to Grubbs's test as outliers – PMe$_3$ (**11**), P(2-MeO-C$_6$H$_4$)$_3$ (**31**) and P(dma)$_3$ (**3**). The latter has a P–N bond, unlike all other phosphanes in Fig. 4, which may be the cause for the deviation. In the case of P(2-MeO-C$_6$H$_4$)$_3$, it is possible that the *ortho*-MeO group forms a specific interaction with Ni-metal, leading inductively to a considerable decrease in TEP value (around 20 cm^{-1}), or the ν(CO) measurements are somehow erroneous.

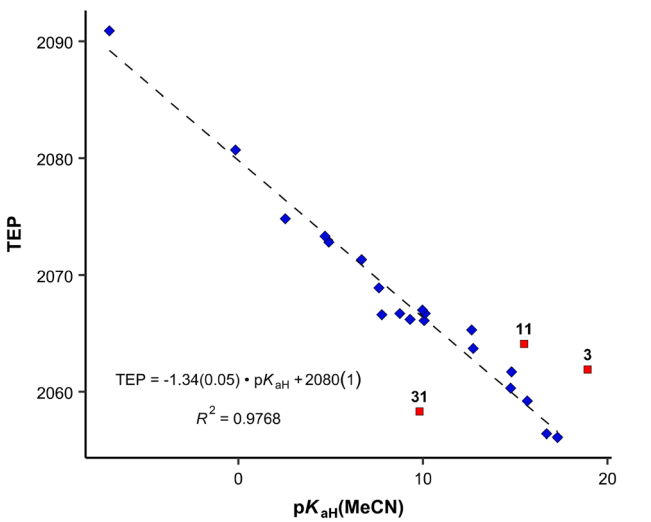

Fig. 4 Correlation between pK_{aH}(MeCN) values and TEP values. Blue diamonds: datapoints included in the correlation denoted by a dashed line; red squares: points omitted from the correlation (outliers according to the Grubbs test).

PMe_3 is the smallest of the studied ligands. The correlation with all points included is presented in the SI. The differences of the correlation coefficients are minor. However, the identities of the outliers give useful information regarding the limits of using this correlation for predictions.

Computational gas-phase proton affinity (PA), similar to the gas-phase basicity (GB) utilized in this study, and HOMO energies have been employed to estimate the suitability of phosphine ligands.[13] However, our findings indicate that gas-phase computational results demonstrate a markedly weaker correlation with solution-phase values like TEP. We observe a considerably weaker correlation between GB and TEP (R^2 = 0.807) compared to pK_{aH} values and TEP (R^2 = 0.977). Moreover, when comparing our calculated parameters to other parameters from the literature (*e.g.*, Tolman cone angle), the correlation tends to be inferior for gas-phase values.

Another crucial factor in ligand screening involves considering the size of a ligand. The range of angles attributed to a single ligand can be quite extensive. This diversity is demonstrated in Fig. 6, where vertical bars represent the ranges of various cone angles reported in the literature, including solid cone angle.[9,30,37]

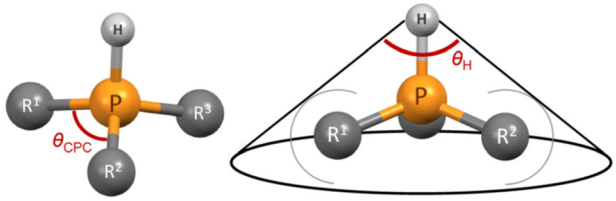

Fig. 5 Single CPC angle (left); the average CPC angle used in this work is calculated using all three single CPC angles. θ_H angle (right) of a phosphane.

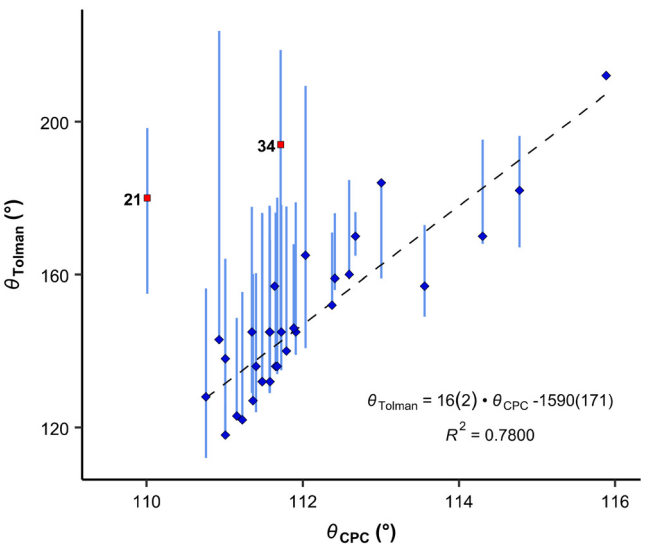

Fig. 6 Correlation between CPC and Tolman angles. Blue diamonds: datapoints included in the correlation denoted by a dashed line; red squares: points omitted from the correlation (outliers according to the Grubbs test). Vertical bars show ranges of various cone angles reported in the literature, including solid cone angle.[9,30,37]

Tolman described that the steric demand of phosphane ligands is poorly characterized by their valence angles (in this work θ_{CPC}).[49] However, we wanted to test whether the CPC angle, determined through a simple and straightforward "three-click method", could offer any reasonable possibility to predict the steric demand of a phosphane and if this simplified method may suffice for preliminary screening purposes. The CPC angle used in this work represents the average of three angles from the most stable conformer of the protonated phosphane (the single CPC angle is depicted in Fig. 5). We opted for the protonated rather than neutral form because it may better represent the structure of the ligand in the metal complex, given the potential influence of the lone pair. However, the CPC angle can also be determined from a neutral phosphane, as it correlates well with the angle observed in its corresponding cation. θ_{CPC} is part of the deformation coordinate S4′,[36] however, the correlation is weak between these two values.

It is apparent that the correlation involving all available compounds would be relatively poor (Fig. 6). We eliminated the most deviating compounds from the correlation. For instance, P(2-Me-C_6H_4)$_3$ (**34**) stands apart from the main group, manifesting a smaller CPC angle than expected. This can be attributed to the orientation of *ortho* methyl groups towards the proton, which allows for the phenyl groups to be compressed (see below). It is conceivable that phosphanes with rigid, sterically cumbersome substituents need to be treated separately from others, although there is not enough data in this study to elaborate on this point. Additionally, it is evident that the CPC and cone angles may not correlate for flexible ligands – significant deviation is observed primarily for PNp_3 (**21**) and, to a lesser extent, for PBn_3 (**32**). Simultaneously, accounting for the diversity reflected in the literature data, as denoted by the vertical bars in Fig. 6, we observe that most of the points fall within the range of various ligand cone angles. The prediction error (RMSD) produced by eqn (6) (composed excluding outliers) over the whole dataset (incl. outliers) is 17 degrees.

$$\theta_{Tolman} = 16(2) \cdot \theta_{CPC} - 1590(171)$$
$$n = 31;\ R^2 = 0.780;\ S = 10 \qquad (6)$$

Moreover, the CPC angle may hold significance as a property for ligands. It has been shown that PNp_3 (**21**) and P(*t*-Bu)$_3$ (**5**) exhibit similar ligand cone angles (180° and 182°, respectively) and electronic properties, but they demonstrate markedly different catalytic properties, particularly concerning bulky substrates.[28]

We see that the CPC method necessitates distinct treatment for different phosphanes. Therefore, we also propose an alternative option that utilizes the exact cone angle concept.[30] In this approach, we calculate the cone angle for the most stable protonated conformer obtained using the COSMO model, utilizing the proton as the apex (Fig. 5); the distance

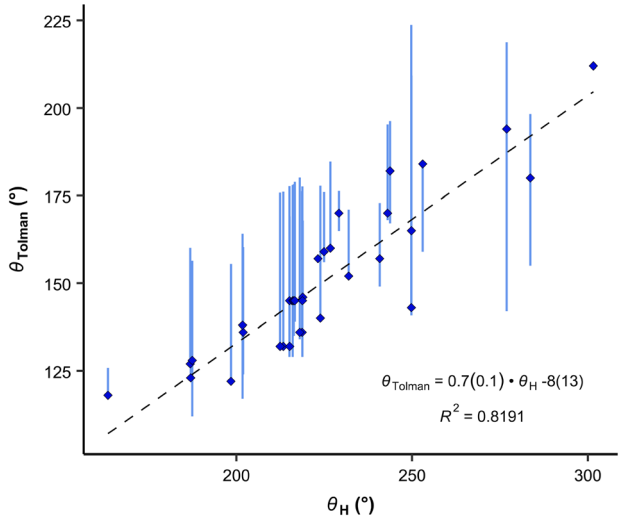

Fig. 7 Correlation between the Tolman cone angles and the exact cone angle of the cation with hydrogen as the apex. Vertical bars show the range of various cone angles reported in the literature, including solid cone angle.[9,30,37]

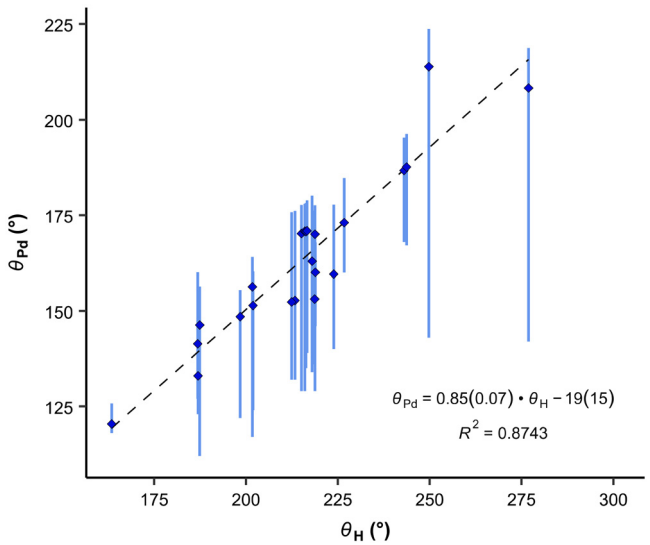

Fig. 8 Correlation between the average exact cone angle of palladium complexes and the exact cone angle of the cation with hydrogen as the apex. Vertical bars show the range of various cone angles reported in the literature, including solid cone angle.[9,30,37]

between P and H atoms comes from the optimized structure and is between 1.409 to 1.422 Å. This angle is denoted as θ_H. Since the proton lies within the van der Waals sphere of phosphorus, phosphorus is, by necessity, ignored in the calculation. Alternatively, the virtual apex point can be moved to the suitable distance along the P–H line. We found the results of both methods to have similar predictive capacity.

The θ_H values correlate relatively well with Tolman cone angle. The θ_H angle of most stable conformer yields to the correlation equation (eqn (7) and Fig. 7):

$$\theta_{Tolman} = 0.7(0.1) \cdot \theta_H - 8(13)$$
$$n = 33;\ R^2 = 0.819;\ S = 10 \quad (7)$$

It is interesting, that the conformers with the smallest θ_H values give only very slightly improved R^2 for the correlation (0.827), but the conformers with the highest energy and largest θ_H angles considerably worsen correlations (R^2 = 0.689 and 0.625, respectively). This demonstrates again, that for fast ligand screening, only the most stable conformer needs to be found.

Our results exhibit a good correlation with the exact cone angles reported in ref. 30 which were calculated for Pd-complexes (denoted in ref. 30 as θ° (Pd) and here as θ_{Pd}). In cases where an exact cone angle was provided for two conformers – with maximum and minimum cone angles – the average values were used for the correlation. The correlation is presented in Fig. 8.

$$\theta_{Pd} = 0.85(0.07) \cdot \theta_H - 19(15)$$
$$n = 23;\ R^2 = 0.874;\ S = 7.9 \quad (8)$$

In the correlation in Fig. 8 and eqn (8), the maximum θ_{Pd} angle, not the average, was used for P(2-Me-C_6H_4)$_3$ (**34**), as the average θ_{Pd} angle does not correlate as well with the θ_H angle of the most stable conformer. The average θ_{Pd} angle of **34** is heavily influenced by the tightest, energetically unfavoured conformer, as it exhibits a more than 40° smaller θ_H angle (Table 3). A similar effect can be observed for the Tolman cone angle (Fig. 6), where **34** is an outlier when the θ_{CPC} angle of the most stable conformer is used. However, if we were to use the tightest conformer, where all Me groups point away from the phosphorus (Table 3), then it would align well with the correlation. For **34**, the variability of the literature values is also

Table 3 Relative energies (ΔE_H) of different conformers of protonated phosphane P(2-Me-C_6H_4)$_3$ (**34**) compared to the most stable conformer and different available angles for 4 different conformers. Relative energies (ΔE_{Pd}) and exact cone angles (θ_{Pd}) of palladium complex of phosphane **34** for 2 different conformers

	All Me groups towards P	Two Me groups towards P	One Me group towards P	No Me groups towards P
ΔE_H [a] [kcal mol^{-1}]	0	1.7	4.7	7.8
θ_{CPC} [°]	111.7	113.1	114.4	115.7
θ_H [°]	276.9	264.2	252.7	236.3
ΔE_{Pd} [kcal mol^{-1}] [b]	0	—	—	12.9
θ_{Pd} [b] [°]	208.2	—	—	175.6
θ_{Tolman} [°]				194[c]

[a] BP86/def-TZVP/COSMO//BP86/def2-TZVPD/COSMO. [b] Ref. 30. [c] Ref. 49; exact conformer not known.

high, which comes from the involvement of different conformers. In principle, this can be the case with all asymmetrically *ortho*-substituted triphenylphoshanes, which have to be treated with caution. Energies and angles for different conformers of **34** are presented in Table 3.

Conclusions

This work provides previously unpublished experimental basicity values for 12 phosphanes measured using either UV-Vis or NMR methods. Computational pK_{aH} values for 56 phosphanes are provided. Furthermore, self-consistent pK_{aH} values of 13 additional phosphanes from the literature are presented. In total, these data cover pK_{aH}(MeCN) values spanning almost 30 orders of magnitude. Steric parameters are also calculated for all 56 phosphanes.

A framework for evaluating the electronic and steric properties of phosphanes is proposed. It is suggested that the conventional Tolman Electronic Parameters (TEP values) could be replaced with pK_{aH} values based on the correlation between the two. The pK_{aH} values are more accessible due to the availability and ease of calculations – obtaining the computational pK_{aH} values is relatively straightforward with the COSMO-RS method, requiring only the identification and optimization of the most stable conformers of neutral and protonated forms. This approach enables facile ligand screening, which considerably simplifies the assessment of phosphanes as potential ligands.

The CPC angles or the exact cone angles of protonated phosphanes (θ_H), depending on the set of phosphanes, may be used instead of various previously utilized cone angles for preliminary screening purposes. The CPC angle serves as the most user-friendly property for ligand size, readily obtainable from the computational or crystal structure of a phosphane. However, it has some limitations, particularly with branched phosphanes. In cases where the CPC angle proves inadequate, θ_H can be employed as an alternative.

This prospective adjustment could streamline ligand screening processes in the future, thereby circumventing the necessity for the computation or preparation of metal-ligand complexes.

Experimental

Instruments and materials

^{1}H spectra for measuring pK_{aH} values of P(dma)$_3$, P(pyrr)$_3$, and PCy$_3$ were recorded on a Bruker Avance III HD spectrometer (700 MHz) in CH_3CN. Bruker Topspin software version 3.2 was used for spectrum processing. ^{1}H chemical shifts were calibrated relative to the solvent peak: CH_3CN/CD_3CN ^{1}H 1.94 ppm. All other pK_{aH}(MeCN) measurements were carried out using UV-Vis spectrometer Lambda 40. The calculations were done using the following software: Avogadro 1.95.0, Tmolex 23.0.0, Turbomole 7.7, COSMOconf 21.0, COSMOtherm 23.0.0, R 4.3.2, and RStudio 2023.12.0. Air- and moisture-sensitive substances were handled in the Vigor SG1200/750TS glovebox. Karl Fischer titration was carried out on the Mettler Toledo DL32 coulometer to determine water content. Acetonitrile (Romil 190 SpS far UV/gradient quality) was used as a solvent for pK_{aH} measurements after drying on molecular sieves (3 Å) for at least 12 hours, which ensured a water content under 6 ppm. All reagents were obtained from commercial sources and used without further purification. The following phosphanes were prepared according to previously described procedures: PMes$_3$,[50,51] P[2,4,6-(MeO)$_3$-C$_6$H$_2$]Ph$_2$, P[2,4,6-(MeO)$_3$-C$_6$H$_2$]$_2$Ph and P[2,4,6-(MeO)$_3$-C$_6$H$_2$]$_3$,[52,53] P(3-MeO-C$_6$H$_4$)$_3$,[54] P[3,5-(MeO)$_2$-C$_6$H$_3$]$_3$,[55,56] PCyPh$_2$,[57] P(1-Napht)Ph$_2$,[58] and P[2,6-(MeO)$_2$-C$_6$H$_3$]$_3$.[52,53,55] Synthesis, purification, and identification of the used noncommercial reference bases are described in ref. 59, 60 and 61. The obtained spectral data corresponded to that previously reported. The preparation of the reference base 4-(Ph-N=N)-C$_6$H$_4$-N=P$_1$(dma)$_2$Ph is detailed in the ESI.†

pK_{aH} measurements

A relative pK_{aH} measurement method was employed to obtain the pK_{aH} values of phosphanes.[44,62,63] In this approach, a base under examination was titrated alongside a reference base within a single solution to ascertain the difference in pK_{aH} values (ΔpK_{aH}).

NMR titration method

Inside a glovebox, three solutions were prepared in vials: (1) basic titrant *t*-Bu-N=P(pyrr)$_3$, (2) acidic titrant CH_3SO_3H, and (3) the substance under investigation + reference(s). Typically, two references were concurrently employed, and the comparison of the obtained difference in pK_{aH} values between these references with the difference of their pK_{aH} values in ref. 44 served as an additional criterion for validating the method. Dry acetonitrile was used as the solvent (CD_3CN was used for PCy$_3$), and the concentrations were in the order of $n \times 10^{-3}$ M for the measured substances and in the order of $n \times 10^{-2}$ M for titrants. The solution containing the bases of interest (0.5 ml) was pipetted into three NMR tubes: two of them were standard NMR tubes, where 0.5 equiv. of basic titrant was added to one and 1.2–1.5 equiv. of acidic titrant to the other to obtain the corresponding (de)protonated forms. The third tube was a J Young NMR guard tube with a 1.5 ml vial cap (with a septum), where titration was later conducted at the NMR machine. Parafilm was applied to all vials and NMR tubes around the caps.

Initially, the spectra of the (de)protonated forms of the bases were measured with NMR, followed by the titration process. Prior to each measurement, shimming was carried out using the MeCN peak to ensure the optimal quality of the peaks. The first spectrum was acquired without the titrant. Titrant was drawn into the syringe from a sealed vial through a septum and added to the NMR tube also through a septum to minimize water content (water content was checked after titration in randomly selected samples and was typically below

10 ppm and never higher than 150 ppm; CD_3CN used for PCy_3 had a higher water content than regularly used CH_3CN). The titrant was added in increments of 2–10 drops depending on the previous spectrum and dissociation levels of the bases. As the peaks of some phosphanes broaden during titration and their chemical shifts cannot always be precisely determined due to overlapping with additional peaks, caution must be exercised during titrant addition to obtain a sufficient number of data points at appropriate dissociation levels.

To calculate the ΔpK_{aH} values, the chemical shifts of the fully protonated forms (δB_1H^+ and δB_2H^+), the fully deprotonated forms (δB_1 and δB_2), and the chemical shifts of the investigated compounds at intermediary states (δ_1 and δ_2) were used (eqn (9)).[43] δ_1 and δ_2 were acquired for each titration point where the chemical shifts correspond to equilibrium mixtures of protonated and deprotonated forms at a given pH (exact pH value is irrelevant). The final ΔpK_{aH} value was averaged over at least three titration points (usually five or more) where $(\delta - \delta B)/(\delta BH^+ - \delta B)$ was between 0.1 and 0.9 for both bases.

$$\Delta pK_{aH} = pK_{aH}(B_1) - pK_{aH}(B_2) = \log\frac{K_{aH}(B_2)}{K_{aH}(B_1)} = \\ = \log\frac{[B_2][B_1H^+]}{[B_1][B_2H^+]} = \log\frac{(\delta_1 - \delta B_1)(\delta B_2H^+ - \delta_2)}{(\delta B_1H^+ - \delta_1)(\delta_2 - \delta B_2)} \quad (9)$$

UV-Vis spectrophotometric titration method

UV-Vis spectrophotometric titration method and setup used in this work is previously published by Saame *et al.*[63] In essence, each base, both the reference and the one under investigation, is individually titrated to obtain UV-Vis spectra for their fully protonated and deprotonated forms. Subsequently, a titration is conducted using a mixture containing both bases. By analyzing the spectral data acquired from this mixture at various wavelengths and employing multilinear regression analysis, the dissociation levels α = [B]/([B] + [BH^+]) of the protonated forms for both bases are determined across all titration mixtures. These α values are then used to calculate the differences of the pK_{aH}(MeCN) values (ΔpK_{aH}) of the two bases according to the following equation:

$$\Delta pK_{aH} = \log\frac{\alpha_1(1-\alpha_2)}{\alpha_2(1-\alpha_1)} \quad (10)$$

The pK_{aH}(MeCN) values were obtained as a result of ΔpK_{aH} measurements against at least three different reference bases. The concentrations of bases in all the solutions were in the order of $n \times 10^{-5}$ M, and the concentrations of the acidic (CH_3SO_3H) and basic (*t*-Bu-N=P(pyrr)$_3$) titrant were in the order of $n \times 10^{-3}$ M.

Calculations

Gas-phase calculations were conducted following the method outlined in ref. 19. Results are presented in ESI.† For HOMO/LUMO energies, single point calculation was carried out at MP2/def2-TZVPP level of theory for the geometries optimized at BP86/def2-TZVP level.

Basicities in solution were estimated by calculating the pK_{aH} values with the COSMO-RS[64–66] method and correcting them using existing experimental data[17,18,67,68] for analogous compounds. In order to calculate the pK_{aH} values with the COSMO-RS method, first, DFT calculations were conducted for multiple conformers of neutral and protonated forms in an ideal conductor, yielding the total energies of the structures alongside partial charge distributions on the molecular surface. These results were then employed as input for statistical thermodynamic calculations, determining the energies of intermolecular interactions within liquid mixtures, as well as the total Gibbs energies of molecules within the liquids.

The conformational search was carried out with COSMOconf[69] software using the def-TZVP basis set (B86 functional) with the COSMO model. Reaching energy minima during geometry optimization was confirmed by calculating the vibrational spectra and ensuring that imaginary frequencies were absent or very small – wavenumbers were in the range of −5 to −36 cm^{-1} for 11 compounds (15 conformers). The effect of remaining imaginary frequencies was less than 0.1 units to the pK_{aH} values. Subsequently, a single point calculation was conducted for all geometries using the def2-TZVPD basis set (BP86 functional), COSMO model, and *Fine* cavity parameter. QM calculations were carried out using TURBOMOLE V7.7.[70] pK_{aH}(MeCN) values were computed using COSMOtherm[71] software (see ESI†). The parameterizations listed in Table 2 were compared for the prediction of pK_{aH} values of phosphanes in acetonitrile. The BP_TZVPD_FINE_C30_1701 parametrization was applied to compute the pK_{aH}(Calc.) values in MeCN, which were then correlated to derive the predicted pK_{aH}(MeCN) values. Every older parameterization used in this work is available with COSMOtherm newer versions. All unique conformers with relative energy below 3 kcal mol^{-1} (when compared to the most stable conformer c0) were considered when calculating the pK_{aH} values.

θ_H angles were calculated numerically by finding the vector of the cone axis using an optimization function (the used code in R language[72] is available in ESI†). The van der Waals radii of the elements were taken from ref. 30.

Data availability

The data that support the findings of this study are available in the ESI† of this article and in Data DOI repository at **https://datadoi.ee/handle/33/604** (**https://doi.org/10.23673/re-461**).[73]

Conflicts of interest

There are no conflicts to declare.

Acknowledgements

This work was supported by grant PRG1736 from the Estonian Research Council and by the grant TK210 from the Estonian Ministry of Education and Research. Research was carried out using the instrumentation at the Estonian Center of Analytical Chemistry (TT4, **https://www.akki.ee**). The quantum-chemical computations were carried out in the High Performance Computing Center of the University of Tartu.[73]

References

1 F. R. Hartley, in *Organophosphorus Compounds*, John Wiley & Sons, Ltd, Chichester, UK, 1990, pp. 1–8.
2 B. T. Elie, C. Levine, I. Ubarretxena-Belandia, A. Varela-Ramírez, R. J. Aguilera, R. Ovalle and M. Contel, *Eur. J. Inorg. Chem.*, 2009, **2009**, 3421–3430.
3 J. Broggi, C. A. Urbina-Blanco, H. Clavier, A. Leitgeb, C. Slugovc, A. M. Z. Slawin and S. P. Nolan, *Chem. – Eur. J.*, 2010, **16**, 9215–9225.
4 D. Amoroso, J. L. Snelgrove, J. C. Conrad, S. D. Drouin, G. P. A. Yap and D. E. Fogg, *Adv. Synth. Catal.*, 2002, **344**, 757–763.
5 R. A. Findeis and L. H. Gade, *Eur. J. Inorg. Chem.*, 2003, **2003**, 99–110.
6 S. T. Nguyen and T. M. Trnka, in *Handbook of Metathesis*, ed. R. H. Grubbs, Weinheim, 2003, pp. 61–85.
7 M.-L. Pikma, M. Ilisson, R. Zalite, D. Lavogina, T. Haljasorg and U. Mäeorg, *Chem. Heterocycl. Compd.*, 2022, **58**, 206–216.
8 W. G. Whitehurst, J. Kim, S. G. Koenig and P. J. Chirik, *J. Am. Chem. Soc.*, 2022, **144**, 4530–4540.
9 W. Matsuoka, Y. Harabuchi, Y. Nagata and S. Maeda, *Org. Biomol. Chem.*, 2023, **21**, 3132–3142.
10 D. W. Stephan, *Chem*, 2020, **6**, 1520–1526.
11 M. N. Hopkinson, C. Richter, M. Schedler and F. Glorius, *Nature*, 2014, **510**, 485–496.
12 F. Fache, E. Schulz, M. L. Tommasino and M. Lemaire, *Chem. Rev.*, 2000, **100**, 2159–2232.
13 N. Fey, A. C. Tsipis, S. E. Harris, J. N. Harvey, A. G. Orpen and R. A. Mansson, *Chem. – Eur. J.*, 2006, **12**, 291–302.
14 T. Gensch, G. dos Passos Gomes, P. Friederich, E. Peters, T. Gaudin, R. Pollice, K. Jorner, A. Nigam, M. Lindner-D'Addario, M. S. Sigman and A. Aspuru-Guzik, *J. Am. Chem. Soc.*, 2022, **144**, 1205–1217.
15 K. Yoshimoto, H. Kawabata, N. Nakamichi and M. Hayashi, *Chem. Lett.*, 2001, **30**, 934–935.
16 M. Fevre, J. Vignolle, V. Heroguez and D. Taton, *Macromolecules*, 2012, **45**, 7711–7718.
17 L. Greb, S. Tussing, B. Schirmer, P. Oña-Burgos, K. Kaupmees, M. Lõkov, I. Leito, S. Grimme and J. Paradies, *Chem. Sci.*, 2013, **4**, 2788–2796.
18 K. Haav, J. Saame, A. Kütt and I. Leito, *Eur. J. Org. Chem.*, 2012, 2167–2172.
19 M.-L. Pikma, M. Lõkov, S. Tshepelevitsh, J. Saame, T. Haljasorg, L. Toom, S. Selberg, I. Leito and A. Kütt, *Eur. J. Org. Chem.*, 2023, e202300453.
20 K. Vazdar, D. Margetić, B. Kovačević, J. Sundermeyer, I. Leito and U. Jahn, *Acc. Chem. Res.*, 2021, **54**, 3108–3123.
21 C. A. Tolman, *J. Am. Chem. Soc.*, 1970, **92**, 2953–2956.
22 C. A. Tolman, *Chem. Rev.*, 1977, **77**, 313–348.
23 G. A. Ardizzoia and S. Brenna, *Phys. Chem. Chem. Phys.*, 2017, **19**, 5971–5978.
24 D. S. Coll, A. B. Vidal, J. A. Rodríguez, E. Ocando-Mavárez, R. Añez and A. Sierraalta, *Inorg. Chim. Acta*, 2015, **436**, 163–168.
25 R. Kalescky, E. Kraka and D. Cremer, *Inorg. Chem.*, 2014, **53**, 478–495.
26 T. E. Müller and D. M. P. Mingos, *Transition Met. Chem.*, 1995, **20**, 533–539.
27 C. A. Tolman, *J. Am. Chem. Soc.*, 1970, **92**, 2956–2965.
28 S. M. Raders, J. N. Moore, J. K. Parks, A. D. Miller, T. M. Leißing, S. P. Kelley, R. D. Rogers and K. H. Shaughnessy, *J. Org. Chem.*, 2013, **78**, 4649–4664.
29 T. E. Barder and S. L. Buchwald, *J. Am. Chem. Soc.*, 2007, **129**, 12003–12010.
30 J. A. Bilbrey, A. H. Kazez, J. Locklin and W. D. Allen, *J. Comput. Chem.*, 2013, **34**, 1189–1197.
31 D. White, B. C. Taverner, P. g. l. Leach and N. J. Coville, *J. Comput. Chem.*, 1993, **14**, 1042–1049.
32 A. C. Hillier, W. J. Sommer, B. S. Yong, J. L. Petersen, L. Cavallo and S. P. Nolan, *Organometallics*, 2003, **22**, 4322–4326.
33 H. Clavier and S. P. Nolan, *Chem. Commun.*, 2010, **46**, 841–861.
34 J. Jover, N. Fey, J. N. Harvey, G. C. Lloyd-Jones, A. G. Orpen, G. J. J. Owen-Smith, P. Murray, D. R. J. Hose, R. Osborne and M. Purdie, *Organometallics*, 2010, **29**, 6245–6258.
35 B. J. Dunne, R. B. Morris and A. G. Orpen, *J. Chem. Soc., Dalton Trans.*, 1991, 653–661.
36 K. D. Cooney, T. R. Cundari, N. W. Hoffman, K. A. Pittard, M. D. Temple and Y. Zhao, *J. Am. Chem. Soc.*, 2003, **125**, 4318–4324.
37 J. Jover and J. Cirera, *Dalton Trans.*, 2019, **48**, 15036–15048.
38 B. Staskun, *J. Org. Chem.*, 1981, **46**, 1643–1646.
39 D. White and N. J. Coville, in *Advances in Organometallic Chemistry*, ed. F. G. A. Stone and R. West, Academic Press, 1994, vol. 36, pp. 95–158.
40 M. Charton, *J. Am. Chem. Soc.*, 1975, **97**, 1552–1556.
41 T. L. Brown and K. J. Lee, *Coord. Chem. Rev.*, 1993, **128**, 89–116.
42 A. Kütt, I. Leito, I. Kaljurand, L. Sooväli, V. M. Vlasov, L. M. Yagupolskii and I. A. Koppel, *J. Org. Chem.*, 2006, **71**, 2829–2838.
43 E. Parman, M. Lõkov, R. Järviste, S. Tshepelevitsh, N. A. Semenov, E. A. Chulanova, G. E. Salnikov, D. O. Prima, Y. G. Slizhov, I. Leito and A. V. Zibarev, *ChemPhysChem*, 2021, **22**, 2329–2335.
44 S. Tshepelevitsh, A. Kütt, M. Lõkov, I. Kaljurand, J. Saame, A. Heering, P. G. Plieger, R. Vianello and I. Leito, *Eur. J. Org. Chem.*, 2019, 6735–6748.

45 A. Klamt, *J. Phys. Chem.*, 1995, **99**, 2224–2235.
46 A. Klamt, F. Eckert and W. Arlt, *Annu. Rev. Chem. Biomol. Eng.*, 2010, **1**, 101–122.
47 M. N. Golovin, M. M. Rahman, J. E. Belmonte and W. P. Giering, *Organometallics*, 1985, **4**, 1981–1991.
48 S. Joerg, R. S. Drago and J. Sales, *Organometallics*, 1998, **17**, 589–599.
49 C. A. Tolman, *Chem. Rev.*, 1977, **77**, 313–348.
50 B. I. Stepanov, E. N. Karpova and A. I. Bokanov, *J. Gen. Chem. USSR*, 1969, **39**, 1514–1519.
51 J. F. Blount, D. Camp, R. D. Hart, P. C. Healy, B. W. Skelton and A. H. White, *Aust. J. Chem.*, 1994, **47**, 1631–1639.
52 I. S. Protopopov and M. Y. Kraft, *Zh. Obshch. Khim.*, 1963, **33**, 3050–3052.
53 M. Wada, S. Higashizaki and A. Tsuboi, *J. Chem. Res., Synop.*, 1985, 38–39.
54 L. Lamza, *J. Prakt. Chem.*, 1964, **25**, 294–300.
55 K. R. Dunbar and S. C. Haefner, *Polyhedron*, 1994, **13**, 727–736.
56 D. Sinou, D. Maillard, A. Aghmiz and A. M. Masdeu i-Bultó, *Adv. Synth. Catal.*, 2003, **345**, 603–611.
57 S. O. Grim, E. F. Davidoff and T. J. Marks, *Z. Naturforsch., B: Anorg. Chem., Org. Chem., Biochem., Biophys., Biol.*, 1971, **26**, 184–190.
58 Y.-L. Zhao, G.-J. Wu, Y. Li, L.-X. Gao and F.-S. Han, *Chem. – Eur. J.*, 2012, **18**, 9622–9627.
59 T. Rodima, V. Mäemets and I. Koppel, *J. Chem. Soc., Perkin Trans. 1*, 2000, 2637–2644.
60 T. Rodima, I. Kaljurand, A. Pihl, V. Mäemets, I. Leito and I. A. Koppel, *J. Org. Chem.*, 2002, **67**, 1873–1881.
61 S. Selberg, T. Rodima, M. Lõkov, S. Tshepelevitsh, T. Haljasorg, S. Chhabra, S. A. Kadam, L. Toom, S. Vahur and I. Leito, *Tetrahedron Lett.*, 2017, **58**, 2098–2102.
62 A. Kütt, S. Selberg, I. Kaljurand, S. Tshepelevitsh, A. Heering, A. Darnell, K. Kaupmees, M. Piirsalu and I. Leito, *Tetrahedron Lett.*, 2018, **59**, 3738–3748.
63 J. Saame, T. Rodima, S. Tshepelevitsh, A. Kütt, I. Kaljurand, T. Haljasorg, I. A. Koppel and I. Leito, *J. Org. Chem.*, 2016, **81**, 7349–7361.
64 A. Klamt, *J. Phys. Chem.*, 1995, **99**, 2224–2235.
65 A. Klamt, V. Jonas, T. Bürger and J. C. W. Lohrenz, *J. Phys. Chem. A*, 1998, **102**, 5074–5085.
66 F. Eckert and A. Klamt, *AIChE J.*, 2002, **48**, 369–385.
67 I. Kaljurand, A. Kütt, L. Sooväli, T. Rodima, V. Mäemets, I. Leito and I. A. Koppel, *J. Org. Chem.*, 2005, **70**, 1019–1028.
68 K. Kaupmees, R. Järviste and I. Leito, *Chem. – Eur. J.*, 2016, **22**, 17445–17449.
69 *BIOVIA COSMOconfX (version 21.0) Dassault Systèmes*, 2021.
70 *TURBOMOLE V7.7 2022, a development of University of Karlsruhe and Forschungszentrum Karlsruhe GmbH, 1989-2007, TURBOMOLE GmbH*, since 2007; available from **https://www.turbomole.org**.
71 *BIOVIA COSMOtherm (version 23.0.0) Dassault Systèmes*, 2023.
72 *R Core Team (2023). R: A language and environment for statistical computing. R Foundation for Statistical Computing*, Vienna, Austria, **https://www.R-project.org/**.
73 *University of Tartu "UT Rocket" share.neic.no*, DOI: **10.23673/PH6N-0144**.